Indian Journal of Chemical Technology
Vol. 31, May 2024, pp. 411-424
DOI: 10.56042/ijct.v31i3.6353

Bacteria against bacteria: Green silver nanoparticle fabrication, antioxidant, anti-biofilm and antibacterial activities

Niloy Chatterjee[1,2], Srija Pal[1,3], Anindita Chakraborty[4] and Pubali Dhar[1,2]*

[1]Laboratory of Food Science and Technology, Food and Nutrition division, University of Calcutta, Kolkata 700 027, West Bengal, India

[2]Centre for Research in Nanoscience & Nanotechnology, University of Calcutta, JD 2, Sector III, Salt Lake City, Kolkata 700 098, West Bengal, India

[3]Department of Chemical Technology, University of Calcutta, Kolkata – 700 009, West Bengal, India

[4]UGC-DAE CSR (Kolkata Centre), Kolkata, 700 098, West Bengal, India

*E-mail: pdhomesc@caluniv.ac.in / pubalighoshdhar@yahoo.co.in

Received 23 October 2023; accepted 30 January 2024

The current study focuses on the assessment of antioxidant and antibacterial properties of Ag nanoparticles (NP) synthesised using a pathogen *Shigella flexneri 29508* in a green synthesis techinque. The synthesis has been confirmed with evolution of surface plasmon resonance band in the absor[ption spectrum of Ag-NPs. The nanosize, homogeneity, and high stability of the particles are confirmed by dynamic light scattering technique. Spherical morphology with an average particle size of 50 nm has been observed by TEM analysis. EDAX clearly demonstrated the presence of elemental silver. Using conventional tests, the antioxidant capacity of the greenly produced Ag-NPs has been assessed. The results showed considerable antioxidant potential, demonstrating the potential of nanoparticles to combat free radicals and guarding against oxidative stress. Additionally, a small number of clinically significant bacterial strains have been used to test the antibacterial effectiveness of the produced Ag-NPs. To assess the detrimental impact of the nanoparticles on bacterial development, Resazurin-based micro-dilution viability test, disc diffusion, and spread plate assay techniques for MIC and MBC determination have been used. The results showed that the tested bacterial infections are resistant to a variety of powerful antibacterial agents in various degrees. Additionally, two biofilm-forming bacterial strains have been used to test the biosynthesized Ag-NPs' biofilm inhibitory and eradicating activities, and the findings demonstrated its powerful anti-biofilm potential. The success of the green synthesis of Ag-NPs utilizing bacteria is highlighted in this study, and their antioxidant, antibacterial, and antibiofilm properties are discussed.

Keywords: Anti-biofilm, Anti-microbial, Anti-oxidative, Green synthesis, Silver nanoparticles

Introduction

Nanotechnology has appeared as a promising field with applications spanning various industries, including healthcare, electronics, energy, and environmental remediation. Among the diverse range of nanoparticles (NPs), a lot of interest has been paid to silver nanoparticles (Ag-NPs) caused by their distinct physical and chemical features and broad-spectrum antimicrobial activity. Traditional methods of Ag-NP synthesis often embrace the utilization of hazardous chemicals and entail energy-intensive techniques, posing challenges in terms of environmental sustainability and safety[1]. The advancement of environmentally conscious methods of synthesis for Ag-NPs has received greater spotlight in recent years, which utilize natural origins, for example, plants, algae, fungi, and bacteria[2]. These eco-friendly approaches offer several advantages, including reduced environmental impact, cost-effectiveness, and the potential to tailor NP properties via selecting biological sources and reaction conditions. Among the various natural sources, bacteria have emerged as promising candidates for the green fabrication of Ag-NPs due to their unique biochemical capabilities and versatility[3].

Ag-NPs synthesis using bacteria involves harnessing the inherent reducing power and enzymatic machinery present in bacterial cells. Bacterial strains are carefully selected based on their ability to produce extracellular or intracellular metabolites that functions as stabilising and reducing components during the generation of nanoparticles[4]. The reduction of silver ions (Ag^+) by bacterial metabolites accelerates the nucleation and subsequent

development of Ag-NPs. The resulting NPs exhibit distinct features, for instance size, shape, and superficial chemistry that determine their overall physicochemical properties and potential applications. Green synthesis using bacteria offers several advantages over conventional chemical methods. Firstly, it provides an environmentally friendly alternative by reducing the practice of hazardous chemicals and minimizing the production of noxious byproducts. Secondly, bacterial synthesis methods are often simple, scalable, and amenable to large-scale production, making them suitable for industrial applications[5]. Thirdly, the presence of biomolecules in bacterial metabolites, such as proteins, enzymes, and polysaccharides, can confer additional functionalities to the synthesized Ag-NPs, such as enhanced stability, biocompatibility, and targeted delivery.

The application of green-synthesized Ag-NPs spans across various fields. In the medical sector, these NPs have demonstrated potent antimicrobial action alongside a widespread variety of microorganisms such as bacteria, fungi, viruses etc. making them promising candidates for developing novel antimicrobials and wound dressings. In the field of catalysis, Ag-NPs have shown remarkable catalytic properties, enabling their use in diverse chemical reactions. Furthermore, the potential applications of green-synthesized Ag-NPs extend to agriculture, including plant disease management, crop enhancement, and environmental remediation[6].

Human health is seriously threatened by infections from bacteria, and managing these illnesses has become more challenging as strains resistant to antibiotics have emerged. Therefore, there is a pressing need to create innovative antibacterial agents with increased effectiveness and decreased tolerance[7]. Ag-NPs have garnered a lot of attention owing to their effectual antibacterial action against a wide variety and types of bacteria, including several modern drug-resistant superbugs. However, conventional methods of Ag-NP synthesis often encourage utilization of menacing chemicals and energy-intensive methods, leading to environmental concerns and safety issues. Numerous pathogenic bacteria, including drug-resistant species, have been subjected to considerable research on the antibacterial effects of green-synthesised Ag-NPs[8]. These NPs exhibit multiple modes of action against bacteria, including destruction to the outer layer of cell membrane layer, intervention with biological and cellular processes, generation of reactive oxygen species (ROS) etc. The tiny size along with large surface area of Ag-NPs facilitates them to interact with bacterial cells, leading to increased antimicrobial efficacy[9]. The potential of benign and eco-friendly silver nanoparticles fabricated using green chemistry, as novel antibacterial agents can be better understood through comprehension of the antibacterial characters of these materials. The unique characteristics of green-synthesized Ag-NPs, combined with their eco-friendly nature, expand new avenues for their usage in fighting against bacterial infections, including drug-resistant strains. Sustained investigation in this domain will bestow to the advancement of effective and sustainable antibacterial strategies, addressing the urgent need for alternative antibacterial agents to combat the growing threat of bacterial infections. The past few years have seen a rise in research in the anti-biofilm activities of green-synthesized Ag-NPs. These NPs have shown efficacy in disrupting biofilm structures, inhibiting biofilm formation, and eradicating mature biofilms. The mechanisms underlying their anti-biofilm activity include physical disruption of biofilm matrices, inhibition of bacterial adhesion, interference with quorum sensing, and upsurge of species of reactive oxygen (ROS)[10]. Deciphering the anti-biofilm potency of green-synthesized Ag-NPs provides valuable insights into their potential as novel strategies to combat biofilm-associated infections[11]. The unique properties of green-synthesized Ag-NPs, combined with their eco-friendly nature, uncover innovative avenues for their utilization in diverse operations, including medical devices, water treatment, and food processing. Continued study in this realm will add to the progress of effective and sustainable anti-biofilm strategies, addressing the urgent need for unconventional techniques to combat biofilm-associated infections.

Experimental Section

Materials

All the chemicals used in experimentation are of analytical reagent category and have been acquired from HiMedia Laboratories (LLC, Pennsylvania) or Sigma Aldrich (United States). Double distilled water and research grade solvents were used throughout the experimental work.

The experimental microbes, *Shigella flexneri 29508*, *Bacillus subtilis 3610*, *E. coli*, *Vibrio cholerae M010 (0139) and Staphylococcus aureus subsp. aureus 6571* were obtained from the Microbial Type

Culture Collection (MTCC) which is housed in the CSIR-Institute of Microbial Technology (IMTech) in Chandigarh, India.

Biosynthesis of Ag-NPs

The pathogenic bacterium *Shigella flexneri 29508* was sub-cultured and stored in the Dept. of Home Science, University of Calcutta, as glycerol stock and agar slants in freezer. With a few minor modifications, the Ameen et al. approach was used for synthesising Ag-NPs[12]. Pure bacterial culture was grown and sub-cultured in nutrient broth media at 37 °C for 20–22 h. The liquid cultures were homogenized for 2 min and thereafter subjected to centrifugation for 8000 rpm at 5 min. Then pellet was discarded and supernatant was kept for further experiment.

For the biogenesis of Ag-NPs, a 250 mL flask containing bacterial extracellular filtrates (10 mL) and aqueous silver nitrate ($AgNO_3$, 3 mM, 90 mL) was mixed thoroughly and kept under dark conditions (RT) for about 24 h. The overt observable colour transition from transparent and colorless to pale yellowish brown to dark brown or black over time, confirmed the synthesis of Ag-NP[13,14]. The Ag-NPs samples were eventually lyophilized in a freeze dryer and kept at 20 °C for later usage shortly after repetitive spinning (16000 rpm and 12 min) and washing the powdered pellet with distilled water.

Physico-chemical characterization

UV-visible spectra investigation

The easiest instrumental method to confirm the fabrication of Ag-NPs is UV-visible spectroscopy. By analysing UV-visible absorption spectra, the initial synthesis of Ag-NPs was confirmed and verified[15]. UV-visible double beam spectrophotometer (Thermo Scientific) was used to measure the light absorption, scanning in a wavelength spectrum of 300 to 800 nm with intermediate resolution of 1 nm range. Double distilled water was used as the reference.

Scanning electron microscopy (SEM) analysis and Energy dispersive X-ray spectroscopy (EDAX)

SEM (SM-1000, Hitachi, Japan), was utilized to observe the surface morphological structure and shape of the fabricated Ag-NPs and documented in accordance with the methodology of Dada et al.,[16]. The sample of dried Ag-NP was mounted on a glass support. To verify the existence of the metallic silver, this instrument also includes a module for energy dispersive X-ray spectroscopy (EDAX). This offers metallic identification of a sample and offers information whether relevant metals are present or not both qualitatively and quantitatively.

Transmission electron microscopic (TEM) observation

The shape, dimension, and structure of the biosynthesized Ag-NPs were characterized by TEM (JEM-1230 TEM, JEOL, Akishima, Japan) functioning at 200 kV. Sample preparation was done utilizing the drop cast technique utilizing a copper mesh grid for 12 h at ambient temperature in order to produce a thin uniform layer. The additional liquid was cleaned and eliminated using a filter paper and organized sequentially in a grid box[17].

Dynamic light scattering (DLS) and zeta potential

The Malvern Zetasizer Nano ZS 6.00 (Malvern Instruments, UK), was used to measure the poly-dispersity index (PDI) and mean hydrodynamic droplet diameter of the synthesized NPs after synthesis. Formulated samples were diluted a hundred times to perform the measurements and in triplicate. Malvern Nano ZS 6.00 (Malvern Instruments, UK) was utilized for measuring zeta potential in order to assess the surface electrical properties or stability of the nanostructures. Using the particle electrophoretic scattering of light effect, surface potential measurements were measured in triplicate[18].

***In vitro* antioxidant potency**

The *in vitro* antioxidant potency of the biosynthesized Ag-NPs was assessed in terms of total content of phenolics, Total content of flavonoids, DPPH (2,2-diphenyl-2-picrylhydrazyl) radical scavenging efficacy, hydrogen peroxide (H_2O_2) scavenging activity, ferrous ion chelating potency, ferric reducing antioxidant power (FRAP) assay, ABTS radical scavenging assay, lipid peroxides radical scavenging capacity, nitric oxide radical scavenging activity and hydroxyl radical scavenging assay. The details of the procedure are given in the Supplementary Information.

***In-vitro* antimicrobial efficacy evaluation**

In-vitro antimicrobial efficacies of bio-fabricated Ag-NPs were assessed in terms of minimum inhibitory concentration (MIC) and minimum bactericidal concentration (MBC). The kinetics assay for antibacterial activity was also performed. *In vitro* biofilm inhibitory activity against bacteria was also measured. The details of all the procedures are given in the Supplementary Information.

Results and Discussion

Biosynthesis and preliminary visual conformation

Fig. 1a shows the precursor solution (i.e. $AgNO_3$) which is transparent, clear and colourless. Thereafter, we can see the reductant (i.e bacterial extracellular culture) with a greenish hue and tinge of grey (Fig. 1b). The Figs (1c-1e) show the colour of the product solution (i.e., Ag-NP). This clearly shows the colour of the resulting $AgNO_3$ solution before and after mixing the bacterial extract completely changed. At the initial phase the colour is light orange however with passage of time the colour deepened and at the end the colour turned deep blackish. According to the study's findings, the shade of the Ag-NPs changed from colourless to light yellow to dark brown after they had been reduced from Ag^+ to Ag^0, which is commonly seen as a sign that NPs were successfully synthesised. With gradual progression of time after mixing of reductant and precursor the colour gradually intensified to dark brownish indicating more profound synthesis of Ag-NPs in the solution.

The reaction solution's colour changes visually, without the need of any instrumentation, from colourless to dark brown, representing the generation of Ag-NPs during the reduction process (Fig. 1) and is the preliminary conformation for such NPs synthesis. Previously similar studies have been conducted and they showed similar phenomenon of change of colour[19]. As the size of NPs are very small, they generally undergo resonance and the electrons present in the nanostructures absorb and scatter light producing different colours of solutions.

Physicochemical characterization

UV-visible spectra analysis

The absorption spectra of the Ag-NPs fabricated with bacterial extracellular extract along with the precursor as well as reductant solution are shown in Fig. 2. The silver nitrate solution as well as the bacterial extracellular extract showed no peak in the absorption spectra. These results suggest that no active components which get excited are present in the salt solution as well as in the extract. However, the spectral scan of Ag-NP solution showed peak around 410 nm due to surface plasmon resonance (SPR). The unbound surface electrons in metal NPs like Ag, when oscillate collectively in resonance with light waves, create a surface plasmon resonance (SPR) absorption band[20]. This new absorption peak appeared after incubation at RT for 2 h. This confirms the reduction Ag^+ to Ag^0 in presence of different phytochemical constituents found in bacterial extract. In line with the findings of this study, earlier investigations indicated that Ag-NPs' absorption peaks ranged from 400 to 450 nm, where they were observed in several experiments at 405, 410, 420, and 426 nm.

DLS (zeta potential and hydrodynamic diameter)

Fig. 3a displays the size dispersal range of biosynthesised Ag-NPs as obtained by DLS. The overall size distribution of Ag-NPs is found to range from 10 to 800 nm. Ag-NPs have an estimated 119.3 nm average particle size distribution. A minor peak of 4555 nm was also found. The polydispersity index (PDI) is found to be 0.229, which indicates a more or less uniform nature of the NPs. The DLS analyzer's wide spectrum reveals that the size of the

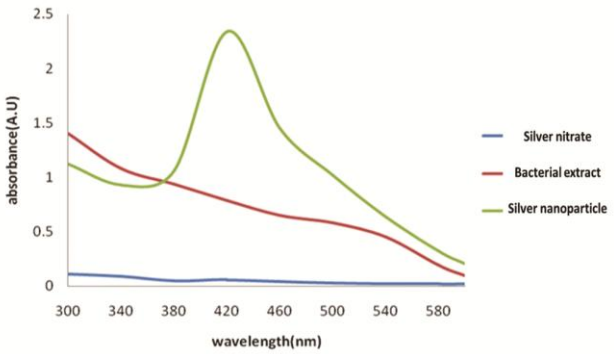

Fig. 2 — UV-visible absorption spectra of silver nitrate, and bacterial extract and Ag-NPs

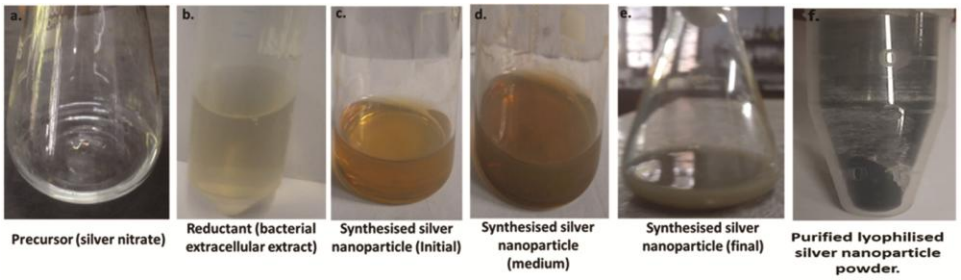

Fig. 1 — Photographs of (a) 3 mM $AgNO_3$ solution, (b) *Shigella flexneri* extracellular bacterial extract. (c-e) Ag-NPs synthesis progression with time (Initial to final) and (f) Final product (Ag nanopowder)

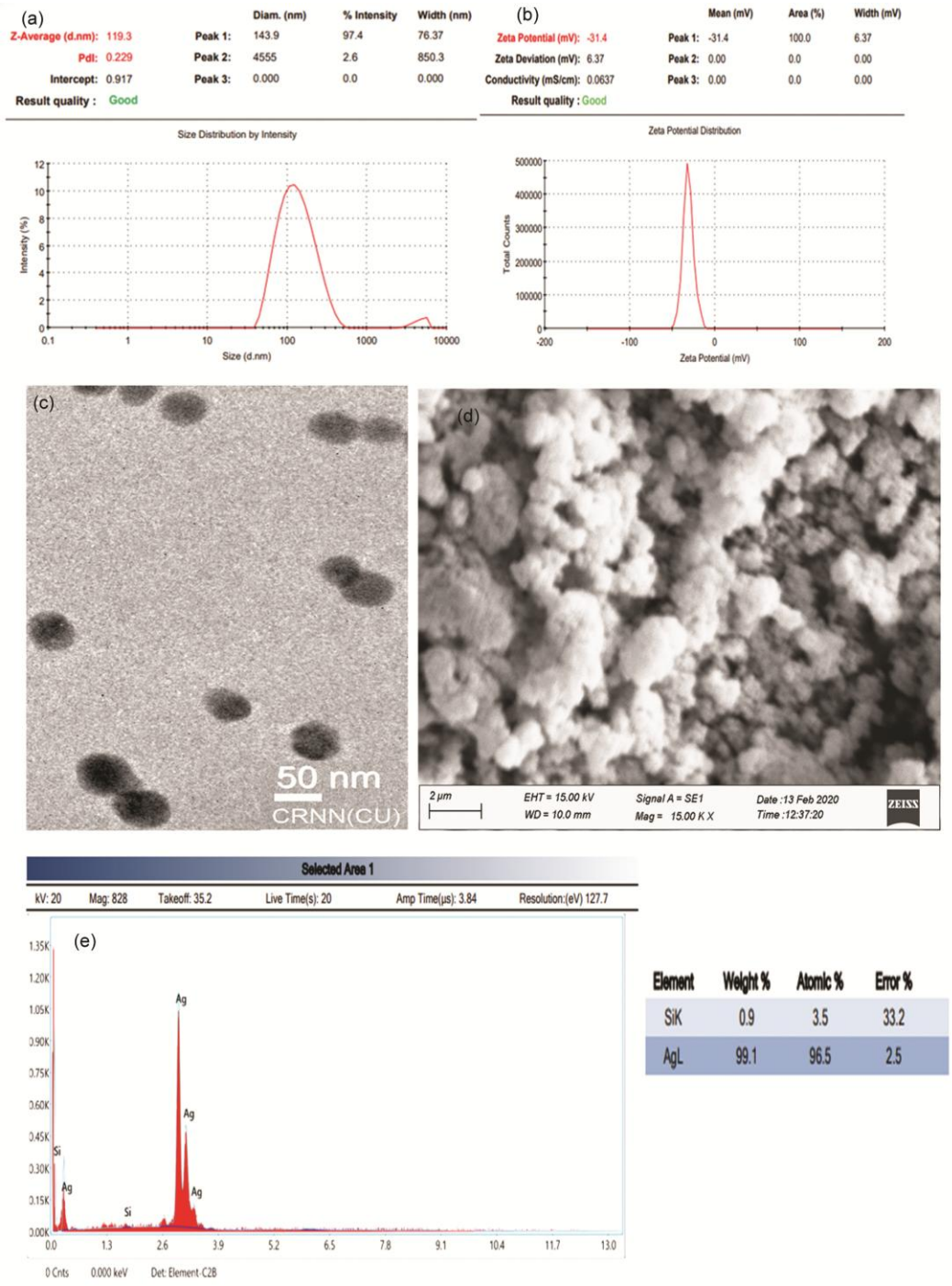

Fig. 3 — (a). Hydrodynamic diameter and homogeneity, (b) Surface charge/zeta potential plot, (c) TEM image, (d) SEM image and (e) EDAX spectrum of the synthesized Ag-NPs

particles has decreased in compared to the absorption spectra's acute SPR signal (424 nm), which indicates a larger particle size. According to previous reports, the typical dimensions of metallic NPs were determined to be in the same range and to have both less and more magnitudes.

The zeta potential curve of biosynthesized Ag-NPs showed a sharp singular spike at -31.4 mV (Fig. 3b). The exteriors of the Ag-NPs are speculated to be highly negative and the core particles to be uniformly dispersed throughout the liquid. The extreme negative magnitude at the surface

demonstrates how strongly attracted and repulsed the particles are to one another. Higher the intensity of negative charge, farther they are from the neutral range suggesting that more extent of opposite charge is required to overcome the barrier and aggregate together.

TEM analysis

The average diameter of the nearly spherical Ag-NPs was found to be 50 nm as shown in the TEM micrograph (Fig. 3c). This finding firmly establishes the possibility that the filtrates from *Shigella flexneri* extracellular media could play a role as not only reducing but also capping agent in the synthesis of Ag-NPs. Saeed et al. also reported the size and shape of Ag-NPs in the similar range using bacteria as the reducing agent[21].

SEM & EDAX analysis

Fig. 3d displays SEM images of Ag-NPs. This shows agglomeration of some spherical particles, which may be due to limited resolution of the SEM technique. Moreover, their sizes are also found within 80 nm. Similar outcomes for various Ag-NPs produced by microbes were also reported by other groups[22].

The EDAX spectrum confirms the presence of metallic Ag as shown in Fig 3e. Inorganic Ag-NPs frequently show an intense signal spike at 3 keV for plasmon resonance at the surface[23]. The EDX method displays the quantitative data of Ag-NPs produced by biosynthesis. The presence of Si in the spectrum may be due to the substrate on which the sample is mounted for the collection of the EDAX spectrum. The bio-fabricated Ag-NPs displayed prominent peak in the 2.5-4 keV region in the present investigation owing to their SPR characteristics. Similar reports were previously found by Kumar & Mamidyala[24] and Kalimuthu et al.[25] and the conformation for the presence of Ag-NPs in the array of 2-4 keV employing *Pseudomonas aeruginosa* and *Bacillus licheniformis* , respectively, as the reducing agent.

Accessment of *in vitro* antioxidant potential

Total phenolics and flavonoids content

The total flavonoid content was 3566.84 μg/mg while the phenolics proportion was 5416.42 μg/mg of the biosynthesized Ag-NPs. The concentrations of both types of phytochemicals are found to be higher than various other previous studies. These phytochemicals indirectly access the antioxidant potential of any system as these chemical constituents helps to relieve oxidative stress. So, from the results it can be said that the green synthesized Ag-NPs from the toxic bacterial strain can be applied in oxidative conditions as counteracting agents. In green synthesized silver suspension flavonoids and polyphenolics were quantified by Firoozi et al.[26] and found to be around 3.758 mg L^{-1} or 0.357 mg g^{-1} and 5.352mg L^{-1} or 0.507 mg g^{-1}, respectively. For the prevention and treatment of degenerative illnesses, flavonoids and phenolic substances demonstrate significant antioxidant activity. Therefore, the increased antiradical activity of these NPs is mostly due to the bioactive chemicals found on their surface.

DPPH radical scavenging activity

In water, methanol, or ethanol, DPPH does not decompose because it is a stable, synthetic radical. The potency of antioxidant substances to neutralize free radicals is influenced by both their ability to donate hydrogen and their overall chemical composition and structure. Ag-NPs were found to have a highly effective DPPH scavenging action. At a very low concentration (18.006 μg mL^{-1}), the Ag-NP removed 50% of free radicals (Table 1). However, all of the utilised conventional antioxidants were more efficient than the NPs. IC_{50} values were around 6.87, 12.85 and 6.94 μg ml^{-1} for BHT, BHA, and Trolox, respectively, which were 61.84%, 28.62%, and 61.45% less than those of Ag-NP. In a different investigation, green synthesised Ag-NPs that demonstrated 91% scavenging action at a 5 g mL^{-1}.

Table 1 — Antioxidant activity of the bio-synthesised Ag-NPs by various *in vitro* methods

In vitro antioxidant potential	BHA	BHT	Trolox	Ag-NPs
DPPH scavenging activity (IC_{50}, μg mL^{-1})	6.871 ±1.554	12.853 ± 0.103	6.94 ±0.100	18.006 ± 0.161
H_2O_2 scavenging activity (IC_{50}, μg mL^{-1})	52.469±0.0021	84.428 ±2.010	60.694±0.468	40.668 ±0.539
Ferrous ion chelating activity (IC_{50}, μg mL^{-1})	39.814±0.016	52.899 ± 0.05	46.722±0.210	41.567±1.464
Ferric reducing antioxidant power ($FeSo_4$ Mole equivalent (M mg^{-1})	0.285±0.0048	0.137±0.0005	0.117±0.012	0.205±0.0121
ABTS radical scavenging assay (IC_{50}, μg mL^{-1})	35.191±0.177	77.914 ±0.521	43.45 ± 0.145	34.482 ± 0.513
Lipid peroxides radical scavenging (IC_{50}, μg mL^{-1})	37.92±0.001	69.1±0.001	52.89±0.29	28.739± 0.032
Nitric oxide radical scavenging activity (IC_{50}, μg mL^{-1})	69.29±0.254	79.418±0.211	73.294±0.492	43.819±0.223
Hydroxyl radical scavenging activity (IC_{50}, μg mL^{-1})	51.153±0.311	82.174±0.029	68.881±1.001	38.478±0.569

Likewise, the Ag-NPs show greater scavanging of DPPH radicals with IC_{50} at very lesser concentrations of 7.03 μg mL^{-1}.

H_2O_2 scavenging activity

Since H_2O_2 typically undergoes auto-degradation, this reagent must be generated quickly and effectively and stored in dark amber vials for antioxidant assays. Ag-NPs were particularly effective at scavenging this radical, showing 50% inhibition at 40.668 μg mL^{-1} concentration (Table 2). It was observed that these NPs showed comparatively more potency than all of the selected control antioxidants. IC_{50} values of BHT, BHA and Trolox were 107.6%, 29.02%, and 49.24% higher than that of Ag-NP. All these standard antioxidants were highly efficient in destroying this radical with 50% inhibitory doses at 84.42, 52.46 and 60.69 μg mL^{-1}.In order to hinder the development of oxidised products in biological systems, these Ag-NPs can be utilized. The effect is mainly due to scavenging activity by transferring electrons to H_2O_2 and neutralizing it into water. Previously, Ag-NPs synthesized using aqueous extract of *Odontonema strictum* showed H_2O_2 IC_{50} scavenging capacity at 4.41 μg mL^{-1}. In another study Ag-NPs fabricated using *Justicia diffusa* as reductant degraded the radical by 96% at 66.6 μg mL^{-1} and about 62 % at 7.40 μg mL^{-1}. Studies of earlier findings have shown that the normal vitamin C has a H_2O_2 scavenging activity of 65.63%, whereas Ag-NPs synthesised by *Cestrum nocturnum* have a H_2O_2 scavenging activity of 45.41%[27].

Ferrous ion chelating activity

Metal-catalyzed oxidation processes require reactive oxygen molecules or species (ROS) as necessary intermediates. The transition metal ion Fe^{2+} can maintain free radical generation by acquiring or losing electrons. Therefore, by chelating metal ions with chelating agents, it is possible to reduce the ROS generation. As a result, many chelation power assays are conducted to evaluate the chelation capacity. In our investigation, the chelation activity of Ag-NP was shown with IC_{50} of 41.56 μg mL^{-1}. BHT exhibited same activity at about 52.89 μg ml^{-1}, while BHA and Trolox did so at 39.81 and 46.72 μg mL^{-1}, respectively (Table 2). The inhibitory amount of standard anti-oxidant BHA was 4.22% lower; while that of BHT and trolox were 27.26 % and 12.4% higher than that of Ag-NP. Prior investigations have demonstrated that iron chelation activity of green synthesized AgNPs at 43.8 μg mL^{-1}[Ref.28].

Table 2 — MIC, MBC values and Tolerance of the bio-synthesised Ag-NPs for different bacterial strains

Bacteria	MIC (μg/mL)	MBC (μg/mL)	Tolerance level	Inference
E.coli	12.5	25	2	Bactericidal
Vibrio cholera	5	20	4	Bactericidal
Staphylococcus aureussubsp.aureus	12.5	30	2.4	Bactericidal
Bacillus subtilis	15	37.5	2.5	Bactericidal

Nitric oxide radical scavenging activity

Free radicals that contain oxygen as well as various chemically active oxygen or nitrogen compounds can be produced by the physiological systems as a byproduct of a variety of biological and biochemical processes. Oxidative stress is primarily formed by oxygen species, although it can also occasionally be caused by nitrogenous radical generation. Similar to other findings, this study demonstrated the ability of Ag-NP to scavenge partially produced nitrite radicals at minute concentration (43.81 μg mL^{-1}), whereas the common antioxidants (BHA, BHT, and trolox) used in this study shown their effectiveness in scavenging free radicals at concentrations of 69.29, 79.41, and 73.29 μg mL^{-1}, respectively. So, the IC_{50} of antioxidants BHA, BHT and trolox were found to be 58.13%, 81.24% and 67.27% more than that of Ag-NP indicating less efficiency. As a result, *in vitro* scavenging of the nitrite anion or other comparable radicals by the control antioxidants was indifferent to practically equally effective. The maximum nitric oxide scavenging rate of 75.06 % was attained at a conc. of 100 μg mL^{-1} Ag-NPs synthesized by *Lactobacillus brevis*[29].

Hydroxyl radical scavenging assay

The utmost physiologically vigorous liberated ionic radical currently recognized *in vivo* in reduced oxygen environments is the hydroxyl radical (•OH). This technique evaluated the capacity of the Ag-NPs to neutralize the supreme adaptable oxidative ion produced in the sub-cellular milieu. While BHT, BHA, and Trolox blocked equimolar concentrations at significantly lower levels of 82.17, 51.15, and 68.88 μg mL^{-1}, respectively, AgNP scavenged 50% of radicals at 38.47 μg mL^{-1}. The IC_{50} concs. of BHA, BHT and Trolox were 32.94%, 113.56% and 79.01% higher than that of the bacterial synthesized Ag-NP. The IC_{50} value for synthesized Ag-NPs' hydroxyl ion destruction efficacy was found to be about 5.08 μg mL^{-1} in earlier investigations. The biosynthesized Ag-NPs had conc. dependent NO

radical destroying efficacy of 78.46% at a higher concentration (100 μg mL^{-1}), which was slightly less than normal BHT (79.11%)[30].

ABTS radical destruction examination

The 50% inhibitory concentration of ABTS cation radical shown by the bacteria synthesized NPs were at 34.48μg mL^{-1}. Alternatively, different standard anti-oxidants BHA, BHT and Trolox inhibited the same amount of free radical damage at 35.19, 77.91 and 43.45 μg mL^{-1}. IC_{50} of BHA, BHT and trolox were 2.06%, 125.96% and 26% higher than that of Ag-NP. So, the green synthesized Ag-NPs were almost similar to BHA and more competent in respect of neutralizing this radical. In another study, AgNPs amalgamated by means of aqueous extracts of *Psidium guajava* L. leaf scavenged 50% radicals at 55.10 μg mL^{-1}. Previous studies conducted using green synthesized Ag-NPs showed that at around 0.5 mg $mL^{-1,}$ the NPs exhibited 88.12% radical exhibiting ability *in vitro*[31]. The process by which NPs possess this free radical scavenging property has important implications for nanomedicine.

Lipid peroxides radical scavenging capacity

The lipid peroxides scavenging capacity of the Ag-NPs were prominent as evidenced from this study. 50% of lipid peroxides were scavenged by 28.739 μg mL^{-1} Ag-NPs. The standard anti-oxidants were able to scavenge the same lipid peroxides at 37.92, 69.1 and 52.89 μg mL^{-1}. The IC_{50} concs. of BHA, BHT as well as trolox were found to be about 32%, 140.44% and 84% higher than that of Ag-NP.

Ferric reducing antioxidant power (FRAP) evaluation

The bacterial synthesized Ag-NPs displayed to be highly active in this assay and showed 0.205 M equivalent of $FeSO_4$ per mg of Ag-NPs. Alternatively, BHA, BHT and Trolox showed 0.285, 0.137 and 0.117 mol equivalent of $FeSO_4$ per mg of sample. Therefore, activity of BHA was found to be 37.56% higher, whereas BHT and trolox were 33.17% and 42.93% lower than that of Ag-NP. Previous studies showed that the FRAP of Ag-NPs increases with concentration and maximum activity was observed of 66.4% at 1 mg mL^{-1}. Again, FRAP of Ag-NPs was found to be around 2.64 M g^{-1}.

***In vitro* antimicrobial efficacy assessment**

Primary antimicrobial activity compared to pathogenic microbes by disc diffusion method

Disc diffusion technique was used on agar plates to gather knowledge about the leading antimicrobial activity of Ag-NPs opposed to pure bacterial pathogens. For simplicity of handling, four different bacterial strains were examined for preliminary antibacterial activity using four concentrations of Ag-NP (2.5, 5, 10 and 20 μg). All four of the pure bacterial cultures exhibited uneven inhibition as determined by inhibition diameters on Petri plates and did not exhibit an expanded inhibition zone with increased concentration (Fig. 4). In *E. coli*, zones of inhibition at lower concentrations of 2.5 and 5 μg were nearly identical (1.21 and 1.08 cm), with the latter demonstrating the least inhibition of all. Besides, 10 and 20 μg showed synchronous increase in inhibition zones with diameters of 1.49 and 2.69 cm, respectively. The 10 μg and 20 μg concentrations increased inhibition by approximately 1.37-fold and 2.5-fold, respectively, than the lowest diameter. Against *V. cholerae*, with increase of concentration the diameter increased gradually. The diameter ranged

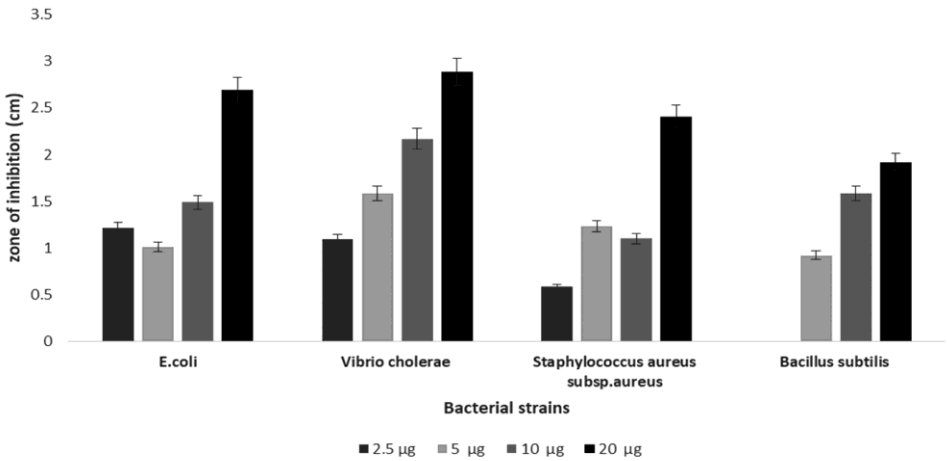

Fig. 4 — Area of mortality of Ag-NPs against bacterial strains by agar plate disc diffusion method

from 1.09 cm to 2.89 cm. 5, 10 and 20 μg NPs showed increase in diameter 1.44 times, 1.99 times and 2.65 times than the lowest one. The *Staphylococcus aureus* bacteria did not show synchronic increase in diameter with concentration. 2.5 μg showed the least activity followed by 10 μg. The 5 μg showed the penultimate inhibition and 10 μg was the highest. The 5 μg showed 2.12 times more inhibition, while 10 μg showed 1.89 times more inhibition and 20 μg 4.15 times more than the lowest inhibition. In *Bacillus subtilis*, the lowest concentration showed no inhibition while with growing concentration of Ag-NPs the diameter gradually increased. The 10 μg showed 1.71 times and 20 μg showed 2.08 times more inhibitory zone than the lowest inhibition diameter. *Bacillus subtilis* at the lowest concentration showed no inhibition. The lowest conc. of *V. cholerae* and 5 μg of *E. coli* showed inhibition diameter in the same range.

At 2.5 μg the order of inhibition found was *V. cholerae*<*E. coli*<*S. aureus*. On the other hand, At 5. 10 and 20 μg the order of inhibitory diameters are: *E. coli* <*S. aureus* <*V. cholera* <*B.subtilis*; *S. aureus* <*B.subtilis*<*E. coli*<*V. cholerae;* and *B.subtilis* < *S. aureus* < *V. cholerae* < *E. coli*, respectively. Therefore, the Ag-NPs were found to be broad-spectrum effectively inhibiting not only Gram-negative but also gram-positive bacteria, with the former pathogens being more vulnerable to suppression than gram-positive counterparts. This could be as a result of a stronger, thicker, external peptidoglycan coating.

Amongst all the highest inhibition was found in *V. cholera* (2.89 cm) and *E. coli* (2.69 cm) at their highest concentrations being followed by highest concentration administered in *S. aureus* (2.41 cm). On the other hand, 5 μg on *V. cholera* and 10 μg on *B. subtilis* as well as 2.5 μg on *V. cholerae*, 10 μg on *S. aureus* and 5 μg on *E. coli* showed similar inhibition. The destruction of cellular membranes by phenolics and NPs and the removal of metals by flavonoids through chelation may have influenced the antibacterial capabilities of the NPs in this research; despite the fact the precise process causing the antimicrobial properties of Ag-NPs is not entirely recognized.

Ag-NPs synthesized using *L. acapulcens* showed the magnitude of the susceptibility over four pathogenic microorganisms of clinical interest. The antimicrobial potency obtained was as follows: $E.\ coli \geq S.\ aureus \geq P.\ aeruginosa > C.\ albicans$. Again, silver nanoparticles synthesized by Bacillus brevis had showed potential antibacterial property against multi-drug resistant pathogens such as *Salmonella typhi* and *Staphylococcus aureus*.

***In vitro* MIC and MBC**

The MIC determines the lowest amount of any antimicrobial test substance that significantly hinders the growth of any pathogen. The concentrations of synthesized Ag-NPs were much less, and found to be within 5-15 μg mL^{-1} for each and every tested bacterium employed in this investigation. The MIC concentrations of Ag-NPs against all the four pathogenic bacteria are depicted in Fig. 5a and Table 2. The MIC against gram negative microorganism *E. coli* was 12.5 μg mL^{-1}, while for *V. cholerae* it was 5 μg mL^{-1}. On the other hand, for gram-positive organisms *S. aureus* MIC was evident at 12.5 μg mL^{-1} and *Bacillus subtilis* 15 μg mL^{-1}. A smaller MIC indicates a more robust and effective antibacterial action because it is well known that MIC measures antimicrobial efficacy[32]. Therefore, the fact that bacteria can be killed or rendered fatal at lower Ag-NP concentrations demonstrates that these nanostructures may prevent bacterial growth and reproduction at very low levels.

The MBC on the other hand represents the lowest level of any antimicrobial test substance that results in the death of the pathogens. Bactericidal efficacy of the inorganic NPs is also highly necessary for any antimicrobial agent as it is the killing or mortality conc. and the most effective amount for carnage of any bacterial species. Besides MIC, this is another important parameter that evaluates at what amount the bacterial growth can be completely inhibited. MBC is generally higher than inhibitory concentration, although in some cases it may be equal to MIC. The Ag-NPs showed MBC at different concentrations for all the chosen strains unlike the MIC. *V. cholerae* showed the least MBC (20 μg mL^{-1}) being followed by *E. coli* (25 μg mL^{-1}) showing that the green synthesized Ag-NPs are highly potent against gram-negative microorganisms. As opposed to that, MBC alongside *S. aureus* and *B. subtilis* were seen to be 30 and 37.5 μg mL^{-1} respectively.

Determination of tolerance level

The ratio of MBC/MIC of any test antimicrobial substance is important in the field of pathogenicity. This ratio is defined as the tolerance level of that agent against a particular pathogen. Lesser the ratio,

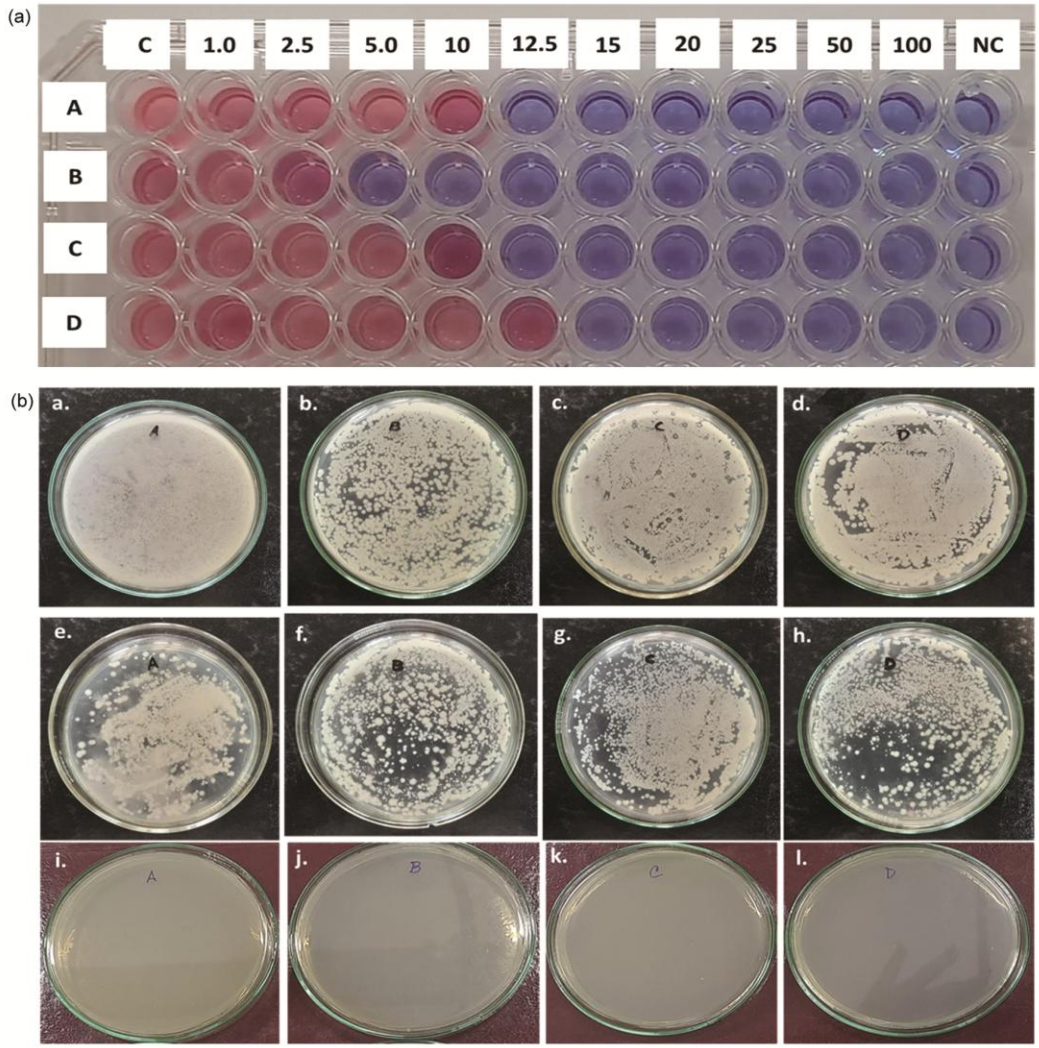

Fig. 5 — (a) MIC determination against bacterial strains by Resazurin based microdilution analysis (A-D= *E. coli, V.cholerae, S. aureus, B. subtilis*) and (b) MBC assessment against bacterial pathogens by spread plate and colony viability assay. (A-D= *E. coli, V.cholerae, S. aureus, B. subtilis*; conc. of Ag-NPs: a-d = 12.5, 5, 12.5, 15 μg mL^{-1} , e-h = 15, 10, 15, 20 μg mL^{-1}, i-l = 25, 20, 30, 37.5 μg mL^{-1})

better is the efficacy of that particular agent. The ratio lessens as MIC and MBC are nearer and are almost in the same range while the ratio widens as the difference between MIC and MBC gradually increases. Less tolerance level is good while increased tolerance level corresponds to less active material. Based on this tolerance level substances are classified as cidal (i.e. it kills the chosen pathogen) or static (i.e. it prevents the growth of pathogens and arrests them in stationary growth phase). Generally ratio threshold of up to 4 is chosen as cidal for any agent and above 4 is chosen as static. In our study, the Ag-NPs showed the ratio or tolerance level within 4 against all the chosen bacterial strains. The least tolerance level was for *E. coli* (2), followed by *S. aureus* (2.46) and *B.subtilis* (2.5) and the least efficacy was found against *V. cholera* (4). Low ratio implies MIC and MBC are very close to each other or very much similar.

Kinetic assay for antibacterial activity

Real time or kinetics of anti-microbial effect of the Ag-NPs was also performed on the bacterial strains. We have chosen three different conc. of Ag-NPs based on their MICs against the chosen pathogens. The concentrations chosen were MIC, 0.5x MIC and 2x MIC. In *E. coli*, at the end of 24 h all the concentrations inhibited growth reducing the bacterial load overall. The killing kinetics assay of Ag-NPs against bacteria is shown in Fig. 6. At 0.5x the growth was initially augmented till 4 h. (0.33) after that it continually declined. The 2x MIC also showed the similar trend (0.27). However MIC treatment

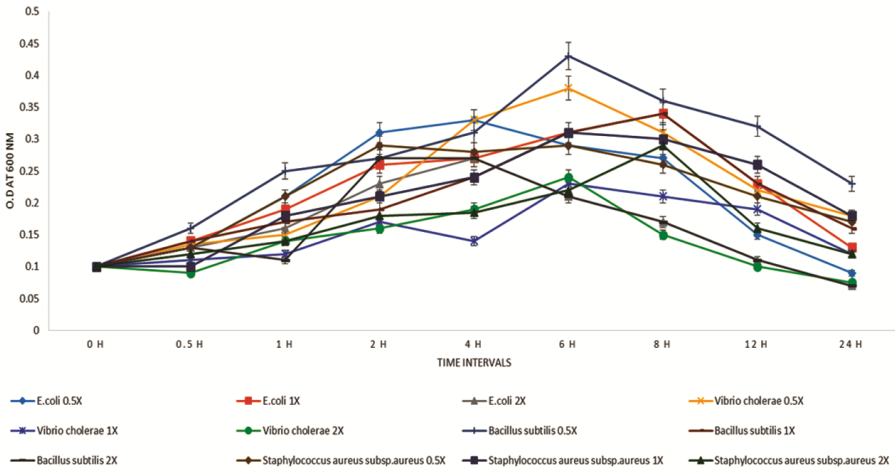

Fig. 6 — Killing kinetics assay of Ag-NPs against bacteria

increased the growth till 8 h. (0.34) and thereafter decreased it till the last. The minimal growths found in all the concentrations against *E. coli* are 0.09, 0.13 and 0.07, respectively. In case of *V. cholerae*, all the three concentrations showed increase in growth till 6 h and after that there is continuous decline in growth trend till 24 h. The 1x and 2x MIC showed almost similar inhibition to that of *E. coli* at the end of 24 h but the 0.5x MIC the growth found was higher. These results suggest that at lower amounts the Ag-NPs are more effective against *E. coli* while at higher amounts the NPs are similarly active against both the gram-negative microbial pathogens.

When gram positive microbes were examined for kinetic antimicrobial activity, the kinetic growth was found to be higher as compared to gram-negative counterparts. In *B. subtilis*, 0.5x and 2x showed increasing growth till 6 h while the 1x increased upto 8 h. The 2x MIC showed the most minimal growth and almost similar to that of the gram-negative organisms. The other two conc. against the chosen bacterial pure culture showed higher growth. Against *S. aureus*, the kinetic trend followed similar to *B. Bacillus*. The *Staphylococcus* was found to be least inhibited in this assay by the green synthesized NPs. At 24 h 0.5x and 1x showed diminished growth but it was much less compared to other bacteria. At 2x MIC amongst all, this bacteria showed the highest growth (0.12).

Determination of mechanism of action on microbes

Ag-NPs tend to damage or break the cell membranes and therefore covering of different cellular structures. The NPs tend to react with different biomolecules present on the cellular surface and thereby causing injury to cell wall as well as cell membrane triggering a wide variety of morphological changes. Due to cell membrane destruction various cellular or intracellular biomolecules get leaked and are released into the extracellular milieu. We tried to measure different prominent biological macro-molecules of the bacteria which can indirectly provide measurement of cell membrane damage by Ag-NPs Four different macromolecules- DNA, protein, total Polysaccharides and Reducing sugars were measured. The membrane leakage assay for mechanism of action of Ag-NPs on bacterial cells is shown in Fig. 7.

DNA was measured using di-phenylamine reagent. In case of *E. coli*, after 2 h. the outflux of DNA increased by 22 %, and after 4 h and 6 h by 38 and 50%, respectively. While *V. cholerae* at 2 h and 4 h less damage occurred resulting in outflux increase by 13 and 23%, respectively. However, at the end of 6 h, DNA in the extracellular medium increased by almost similar to *E. coli* (44 %). For *S. aureus* in the initial 2 h and 4 h damage was noticeable, however, in the final 2 h it increased very less. In *B. subtilis* the least damage was observed. The difference was almost synchronous in the time intervals.

Protein leakage was also measured in the extracellular medium in similar way to determine the membrane rupturing efficacy of the Ag-NPs. In *E.coli*, protein leakage increased by 16%, 24% and 39% after 2, 4 and 6 h, respectively compared to initial time. In *V.cholerae*, same increasing trend was observed and outflow increased by 21, 27 and 35%, respectively, in comparison to 0 h. In *S.aureus*, extracellular protein flex increased by 18, 29 and 38%, respectively. In *B. subtilis*, leakage led to upsurge in protein amounts in extracellular medium

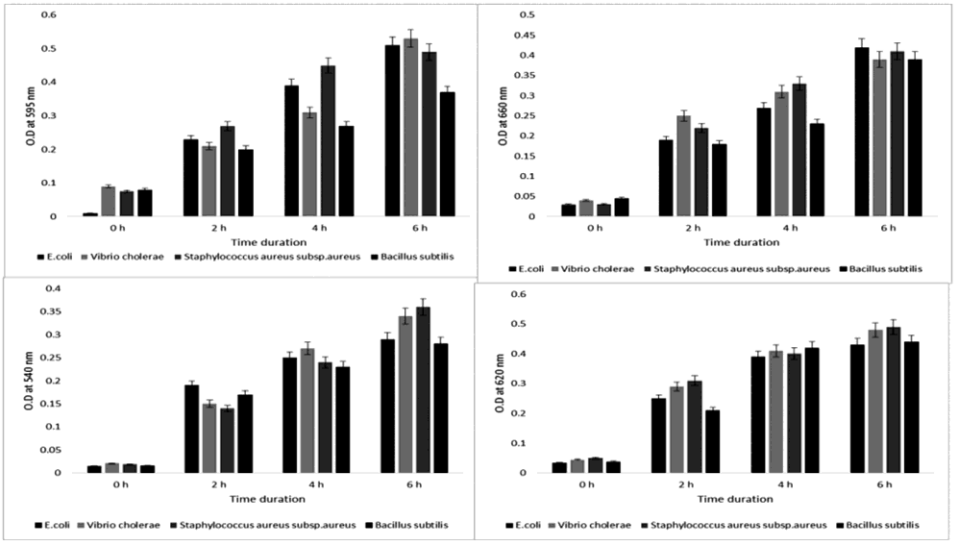

Fig. 7 — Membrane leakage assay for mechanism of action of Ag-NPs on bacterial cells

by 13.5, 18.5 and 33.5 % respectively. The minimum leakage was obtained in *B. subtilis* while highest was observed in *E. coli*.

Sugars and polysaccharides are another important class of biological macromolecules that represent a major cellular fraction. So, in this assay, the outflow of reducing sugars as well as total polysaccharide from the cellular milieu was measured spectrophotometrically. The highest amount of reducing sugars outflow was noticed in *S. aureus* while the least in *B. subtilis*. The gram-negative organisms (i.e., *E.coli* and *V. cholerae*) showed synchronous increase of biomolecule in extracellular phase by 17.5, 23.5, 27. 5% and 12.9, 24.9, 31.9% at 2, 4 and 6 h, respectively. The gram-positive organisms on the other hand, *S. aureus* increased leakage tendency by 12.9, 22.1 and 33.9% respectively, along with *B. subtilis* showed upsurge of 15.4, 21.4 and 26.4%, respectively. The total polysaccharides also showed the similar trend in the experiments. *E. coli* showed increased amount of sugars in the extracellular medium by 21.6, 35.6 and 39.6% while *V. cholerae* showed an increase in extracellular polysaccharides by 24.5, 36.5 and 43.5% after 2, 4 and 6 h, respectively. For *S.aureus*, extracellular biomolecule increased by about 26, 35 and 44% after 2, 4 and 6 h, respectively, while, for *B. subtilis* 17.2, 38.2 and 40.2% at the same time intervals.

In vitro biofilm inhibition

The development of biofilms is a typical method for bacteria to survive in harsh conditions, which enables them to colonize various surfaces and establish complex multicellular communities. Biofilms pose a significant challenge in various settings, including medical devices, water systems, and food processing, as they are highly resistant to traditional antimicrobial treatments and host immune responses. Consequently, there is a serious necessity for the improvement of effective approaches to fight biofilm-associated infections.

We studied the biofilm inhibitory potential of the synthesized Ag-NPs against two bacterial pathogens (Fig. 8a). Ag-NPs inhibited both the bacterial films and with increasing conc. the inhibitory potential increased synonymously upto the penultimate conc. but decreased at the final one. The biofilm production decreased gradually with passage of time indicating that against both the strains biofilm can be greatly repressed. In absence of test substance biofilm formation was found to be about 90% in both the bacteria. In *V. cholerae* at 0.5 μg mL^{-1} biofilm was inhibited by 3.8%, 1 μg mL^{-1} inhibits 13.1%, 2 μg mL^{-1} inhibits 36%, 4 μg mL^{-1} inhibits 61.3%, 8 μg mL^{-1} inhibits 68.8%, 16 μg mL^{-1} inhibits 79.3% and 32 μg mL^{-1} inhibits 75.8% in comparison to the control. The bacterium *S. aureus*, also exhibited the parallel trend and the inhibition increased till penultimate conc. and then decreased. At 0.5 μg mL^{-1} biofilm was inhibited by 5.5 %, 1 μg mL^{-1} inhibits 13.3%, 2 μg mL^{-1} inhibits 30.1%, 4 μg mL^{-1} inhibits 48.9%, 8 μg mL^{-1} inhibits 59.9%, 16 μg mL^{-1} inhibits 74.2% and 32 μg mL^{-1} inhibits 78% in comparison to the control. MBIC (I%>50) values for *V. cholerae* and *S. aureus* were 4 and 8 μg mL^{-1}, respectively.

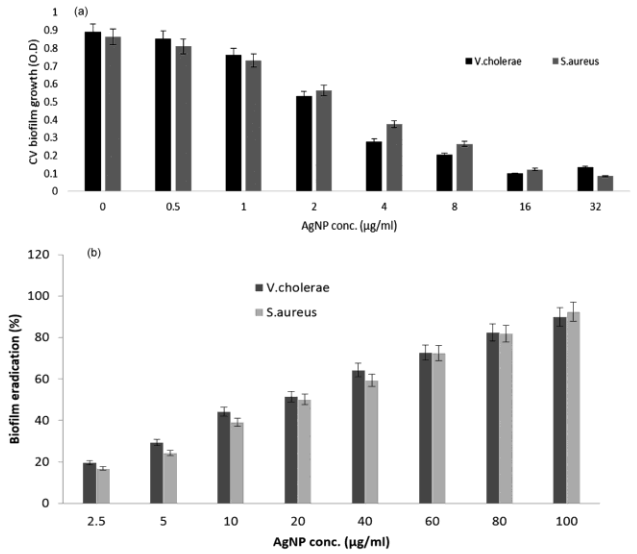

Fig. 8 —Biofilm (a) inhibitory and (b) eradication activity of biosynthesized Ag-NPs

The biofilm eradicatory potential was also studied besides inhibitory activity of the benign and green chemistry fabricated nanoparticles in contrast to two bacterial pathogens was also studied (Fig. 8b). The Ag-NPs inhibited both the bacterial films and with increasing conc. the eradication potential increased synonymously unlike the inhibitory efficacy. The biofilm production decreased gradually with passage of time indicating that against both the strains biofilm can be greatly destroyed. In *V. cholerae* at 2.5 µg mL^{-1} biofilm was eradicated by 19.65%, 5 µg mL^{-1} eradicated 29.47%, 10 µg mL^{-1} eradicates 44.18%, 20 µg mL^{-1} eradicates 51.46%, 40 µg mL^{-1} eradicates 64.32%, 60 µg mL^{-1} eradicates 72.66%, 80 µg mL^{-1} inhibits 82.46% and 100 µg mL^{-1} eliminates 89.92% of the biofilm. The bacterium *S. aureus*, also showed the similar trend and with increase of amount the eradication surged. At 2.5 µg mL^{-1} biofilm was eradicated by 16.88%, 5 µg mL^{-1} eradicated 24.31%, 10 µg mL^{-1} eradicates 39.22%, 20 µg mL^{-1} eradicates 50.18%, 40 µg mL^{-1} eradicates 59.32%, 60 µg mL^{-1} eradicates 72.44%, 80 µg mL^{-1} inhibits 81.88% and 100 µg mL^{-1} eliminates 92.45% of the biofilm. MBEC (E%>50) values for *V. cholerae* and *S. aureus* were 20 µg mL^{-1} for both.

Conclusion

Through this study, it is evident that these biogenic silver nanoparticles exhibit potent antibacterial effects, effectively inhibiting the growth and proliferation of bacteria. Additionally, their ability to combat biofilm formation, a common defense mechanism employed by bacteria, further underscores their potential in combating bacterial infections. Furthermore, the antioxidant activity demonstrated by these Ag-NPs highlights their potential therapeutic applications beyond their antimicrobial properties. Their capacity to destroy damaging oxidative radicals and mitigate oxidative pressure holds promise in numerous medical and industrial applications, including wound healing, drug delivery systems, and cosmetics. In the face of increasing antibiotic resistance and the need for novel therapeutic strategies, the findings presented here shed light on the potency of bacterial-synthesized Ag-NPs as a valuable addition to the arsenal against bacterial infections and oxidative stress-related disorders. However, further studies are warranted to delve deeper into their mechanisms of action, safety profiles, and potential interactions with biological systems, paving the way for their eventual translation into real-world applications that can revolutionize healthcare and industry.

Acknowledgments

The University Grants Council Department of Atomic Energy-Council for Scientific Research (UGC-DAE-CSR) sanctioned vide-UGC-DAE-CSR-KC/CRS/15/IOP/06/0745, New Delhi, provided funding for this study by awarding Niloy Chatterjee with a scholarship for his doctorate research, and the researchers acknowledge them for their assistance.

Supplementary Information

Supplementary information is available on the website http://nopr.niscpr.res.in/handle/123456789.

References

1 Samuel M S, Ravikumar M, John J A, Selvarajan E, Patel H, Chander P S, Soundarya J, Vuppala S, Balaji R & Chandrasekar N, A review on green synthesis of nanoparticles and their diverse biomedical and environmental applications. *Catalysts*, 12 (2022) 459.

2 Velusamy P, Kumar G V, Jeyanthi V, Das J & Pachaiappan R, Bio-inspired green nanoparticles: Synthesis, mechanism, and antibacterial application, *Toxicol Res*, 32 (2016) 95.

3 Kotcherlakota R, Das S & Patra C R, Therapeutic applications of green-synthesized silver nanoparticles, *Green Synth Charact Appl Nanoparticles*, (2018) 389.

4 Narayanan K B & Sakthivel N, Biological synthesis of metal nanoparticles by microbes, *Adv Colloid Interface Sci*, 156 (2010) 1.

5 Abbasi E, Milani M, Aval S F, Kouhi M, Akbarzadeh A, Nasrabadi H T, Nikasa P, Joo S W, Hanifehpour Y, Nejati-

Koshki K & Samiei M, Silver nanoparticles: Synthesis methods, bio-applications and properties, *Crit Rev Microbiol*, 42 (2016) 173.
6 Rauwel P, Rauwel E, Ferdov S & Singh M P, Silver nanoparticles: Synthesis, properties, and applications, *Adv Mater Sci Eng*, 2015 (2015) 624394.
7 Prestinaci F, Pezzotti P & Pantosti A, Antimicrobial resistance: A global multifaceted phenomenon, *Pathog Glob Health*, 109 (2015) 309.
8 Aziz N, Pandey R, Barman I & Prasad R, Leveraging the attributes of mucor hiemalis-derived silver nanoparticles for a synergistic broad-spectrum antimicrobial platform, *Front Microbiol*, 7 (2016) 01984.
9 More P R, Pandit S, Filippis A D, Franci G, Mijakovic I & Galdiero M, Silver nanoparticles: Bactericidal and mechanistic approach against drug resistant pathogens, *Microorganisms*, 11 (2023) 369
10 Joshi A S, Singh P & Mijakovic I, Interactions of gold and silver nanoparticles with bacterial biofilms: Molecular interactions behind inhibition and resistance, *Int J Mol Sci*, 21 (2020) 1.
11 Swidan N S, Hashem Y A, Elkhatib W F & Yassien M A, Antibiofilm activity of green synthesized silver nanoparticles against biofilm associated enterococcal urinary pathogens, *Sci Rep*, 12 (2022) 3869.
12 Ameen F, AlYahya S, Govarthanan M, ALjahdali N, Al-Enazi N, Alsamhary K, Alshehri W A, Alwakeel S S & Alharbi S A, Soil bacteria cupriavidus sp. mediates the extracellular synthesis of antibacterial silver nanoparticles, *J Mol Struct*, 1202 (2020) 127233.
13 Swamy M K, Akhtar M S, Mohanty S K & Sinniah U R, Synthesis and characterization of silver nanoparticles using fruit extract of Momordica cymbalaria and assessment of their in vitro antimicrobial, antioxidant and cytotoxicity activities, *Spectrochim Acta Part A*, 151 (2015) 939.
14 Das V L, Thomas R, Varghese R T, Soniya E V, Mathew J, Radhakrishnan E K, Extracellular synthesis of silver nanoparticles by the Bacillus strain CS 11 isolated from industrialized area, *3 Biotech*, 4 (2014) 121.
15 Logeswari P, Silambarasan S & Abraham J, Ecofriendly synthesis of silver nanoparticles from commercially available plant powders and their antibacterial properties, *Sci Iran*, 20 (2013) 1049.
16 Dada A O, Inyinbor A A, Idu E I, Bello O M, Oluyori A P, Adelani-Akande T A, Okunola A A & Dada O, Effect of operational parameters, characterization and antibacterial studies of green synthesis of silver nanoparticles using Tithonia diversifolia, *Peer J*, 6 (2018) 5865.
17 Chowdhury N R, MacGregor-Ramiasa M, Zilm P, Majewski P & Vasilev K, Chocolate silver nanoparticles: Synthesis, antibacterial activity and cytotoxicity, *J Colloid Interface Sci*, 482 (2016) 151.
18 Anandalakshmi K, Venugobal J & Ramasamy V, Characterization of silver nanoparticles by green synthesis method using pedalium murex leaf extract and their antibacterial activity, *Appl Nanosci*, 6 (2016) 399.
19 Shanmugam R, Chelladurai M, Paulkumar K & Vanaja M, Intracellular and extracellular biosynthesis of silver nanoparticles by using marine bacteria vibrio alginolyticus, *An Int J*, 3 (2013) 21.
20 Smitha S L, Nissamudeen K M, Daizy P & Gopchandran K G, Studies on surface plasmon resonance and photo-luminescence of silver nanoparticles, *Spectrochim Acta Part A*, 71 (2007) 186.
21 Saeed S, Iqbal A & Ashraf M A, Bacterial-mediated synthesis of silver nanoparticles and their significant effect against pathogens, *Environ Sci Pollut Res*, 27 (2020) 37347.
22 Chrakanth R K, Ashajyothi C, Oli A K & Prabhurajeshwar C, Potential bactericidal effect of silver nanoparticles synthesised from Enterococcus species, *Orient J Chem*, 30 (2014) 1253.
23 Sunkar S & Nachiyar C V, Biogenesis of antibacterial silver nanoparticles using the endophytic bacterium Bacillus cereus isolated from Garcinia xanthochymus, *Asian Pac J Trop Biomed*, 2 (2012) 953.
24 Kumar C G & Mamidyala S K, Extracellular synthesis of silver nanoparticles using culture supernatant of Pseudomonas aeruginosa, *Colloids Surf B*, 84 (2011) 462.
25 Kalimuthu Kandasamy, Panneerselvam Chellasamy, Chou Chi, Showe-Mei Lin, Tseng Li-Chun, Tsai Kun-Hsien, Murugan Kadarkarai & Hwang Jiang-Shiou, Predatory efficiency of the copepod Megacyclops formosanus and toxic effect of the red alga Gracilaria firma-synthesized silver nanoparticles against the dengue vector Aedes aegypti." *Hydrobiologia*, 785 (2017) 359.
26 Firoozi S, Jamzad M & Yari M, Biologically synthesized silver nanoparticles by aqueous extract of Satureja intermedia C.A. Mey and the evaluation of total phenolic and flavonoid contents and antioxidant activity, *J Nanostructure Chem*, 6 (2016) 357.
27 Keshari A K, Srivastava R, Singh P, Yadav V B & Nath G, Antioxidant and antibacterial activity of silver nanoparticles synthesized by Cestrum nocturnum, *J Ayurveda Integr Med*, 11 (2020) 37.
28 Bhattacharjee S, Ghosh C, Sen A & Lala M, Characterization of firmiana colorata (Roxb.) R. Br. leaf extract and its silver nanoparticles reveal their antioxidative, anti-microbial, and anti-inflammatory properties, *Int Nano Lett*, 13 (2023) 235.
29 Riaz-Rajoka M S, Mehwish H M, Zhang H, Ashraf M, Fang H, Zeng X, Wu Y, Khurshid M, Zhao L & He Zhendan, Antibacterial and antioxidant activity of exopolysaccharide mediated silver nanoparticle synthesized by Lactobacillus brevis isolated from Chinese koumiss. *Colloids Surf B*, 186 (2020) 110734.
30 Govindappa M, Hemashekhar B, Arthikala M K, Ravishankar R V & Ramachandra Y L, Characterization, antibacterial, antioxidant, antidiabetic, anti-inflammatory and antityrosinase activity of green synthesized silver nanoparticles using Calophyllum tomentosum leaves extract, *Results Phys*, 9 (2018) 400.
31 Sathishkumar R S, Sundaramanickam A, Srinath R, Ramesh T, Saranya K, Meena M & Surya P, Green synthesis of silver nanoparticles by bloom forming marine microalgae Trichodesmium erythraeum and its applications in antioxidant, drug-resistant bacteria, and cytotoxicity activity, *J Saudi Chem Soc*, 23 (2019) 1180.
32 Mueller M., de la Peña A & Derendorf H, Issues in pharmacokinetics and pharmacodynamics of anti-infective agents: Kill curves versus MIC, *Antimicrob Agents Chemother*, 48 (2004) 369.